Available online at www.sciencedirect.com
ScienceDirect
Journal of Photochemistry and Photobiology A: Chemistry 193 (2008) 1–9
Journal of Photochemistry and Photobiology A:Chemistry
www.elsevier.com/locate/jphotochem

Phototransformation of monuron induced by nitrate and nitrite ions in water: Contribution of photonitration

S. Nélieu, M.V. Shankar, L. Kerhoas, J. Einhorn *

INRA, Unité de Phytopharmacie et Médiateurs Chimiques, Route de St-Cyr, 78026 Versailles Cedex, France

Received 29 March 2007; received in revised form 29 May 2007; accepted 30 May 2007
Available online 2 June 2007

Abstract

The nitrate and nitrite-induced phototransformation of monuron in aqueous solution has been investigated using 300–450 nm light irradiation. The degradation kinetics was estimated under various conditions of concentrations of substrate and inducer, oxygen content and pH. From the numerous photoproducts identified using LC–ESI-MS–MS and their evolution curves a degradation scheme was proposed. Besides oxidation of the N-terminus group (major pathway in the presence of NO_3^-) and a minor contribution of direct photolysis, the other photoproducts originated from Cl/OH substitution, regiospecific hydroxylation and/or nitration of the phenyl ring. The two last processes occurred competitively under the NO_3^- conditions even at "environmental" concentrations of the inducer yielding significant levels of nitro-derivatives. Their production was found to be oxygen-dependent in contrast to the NO_2^- conditions.

Keywords: Monuron; Nitrate; Nitrite; Induced phototransformation; Photonitration

1. Introduction

Substituted phenylureas constitute a group of herbicides widely used for general weed control of non-crop area and as pre-emergence treatment on cereals and vegetable crops. Due to their persistence (*ca.* weeks or months) they represent a risk of contamination for natural waters. It is further admitted that transformation products have now to be considered for risk assessment which give rise to an increasing amount of studies. This work is focused on the induced photodegradation of monuron used herein as a representative model due to its known characteristics in water and soil [1,2] and relatively simple structure. Such process is supposed to be competitive with biodegradation [3], whereas hydrolysis, another abiotic event, is unlikely to take place under environmental conditions [4].

Direct photolysis of monuron has been studied in water under UV, solar and simulated solar irradiations. The absorption spectrum of monuron shows a maximum at 245 nm (ε 17,800 L mol^{-1} cm^{-1}) and a weak band at 280 nm. The small overlap with sunlight spectrum ($\lambda > 300$ nm) may lead to a weak degradation [5]. Under UV and low substrate concentration, the main photoproduct results from the substitution of chlorine by a hydroxyl group [6], whereas biphenyl derivatives can be formed at high concentration [7]. The N-terminal substituent may be oxidised to some extent to give demethylation and intermediates. In some conditions the C–Cl bond can be reduced particularly in the presence of methanol or surfactants [8,9].

The photodegradation of monuron can also be induced by photocatalysis, iron salts or humic substances. The heterogeneous TiO_2 photocatalysis is known to proceed through the generation of $^{\bullet}OH$ radicals and positive holes (h^+) on the semiconductor surface. In the case of monuron, this process leads to the formation of *N*-demethylated products, chlorophenyl-isocyanate, chlorophenols, chloroaniline and finally mineralization [10,11]. In the presence of aqueous iron(III) species (particularly $Fe(OH)^{2+}$) which also produce $^{\bullet}OH$ radicals, monuron was shown to undergo mineralization as well [12]. Humic and fulvic acids can induce the degradation of the pesticide through energy transfer (sensitization) or hydrogen atom transfer from their excited triplet states [13]. Both these reactions yield Cl/OH substitution. Nitrates have also been shown to induce photodegradation of phenylureas [14,15]. But no study on the fate of monuron has been reported in this context.

* Corresponding author. Tel.: +33 1 30 83 31 20; fax: +33 1 30 83 31 19.
E-mail address: einhorn@versailles.inra.fr (J. Einhorn).

1010-6030/$ – see front matter © 2007 Elsevier B.V. All rights reserved.
doi:10.1016/j.jphotochem.2007.05.027

Sunlight irradiation of nitrate ions, which are often present in natural waters, gives rise to the reactive $^{\bullet}OH$ radicals, and to $NO_2^{\bullet}$ and N_2O_4 species through reactions (1)–(4) [16,17]. The nitrite ions resulting from reaction (3) or from the photodegradation of humic substances [18] are usually present too, but at lower concentrations. However, NO_2^- can absorb solar radiation more efficiently (NO_2^-: λ_{max} 352 nm, ε 22 L mol^{-1} s^{-1} *versus* NO_3^-: λ_{max} 302 nm, ε 7 L mol^{-1} s^{-1}) and produce subsequently reactive species (Eqs. (5)–(8)) with higher quantum yields [19]. Conversely, NO_2^- can also be regarded as a scavenger towards hydroxyl radicals (Eq. (9)).

$$NO_3^- + h\nu \rightarrow {}^{\bullet}NO_2 + O^{\bullet -} \quad [\Phi_1\,(305\text{–}313\,\text{nm}) = (0.009\text{–}0.017)] \tag{1}$$

$$O^{\bullet -} + H^+ \leftrightarrows {}^{\bullet}OH \quad [pK_a = 11.9] \tag{2}$$

$$NO_3^- + h\nu \rightarrow NO_2^- + O(^3P) \quad [\Phi_2\,(305\,\text{nm}) = 0.001] \tag{3}$$

$$^{\bullet}NO_2 + {}^{\bullet}NO_2 \rightarrow N_2O_4 \quad [k = 4.5 \times 10^8\,\text{L mol}^{-1}\,\text{s}^{-1}] \tag{4}$$

$$NO_2^- + h\nu \rightarrow {}^{\bullet}NO + O^{\bullet -} \quad [\Phi_3\,(355\,\text{nm})\,0.02\text{–}0.07] \tag{5}$$

$$NO_2^- + h\nu \rightarrow {}^{\bullet}NO_2 + e^-_{aq} \quad [\Phi_4\,(355\,\text{nm})\,0.076] \tag{6}$$

$$e^-_{aq} + O_2 \rightarrow O_2^{\bullet -} \quad [k = 1.9 \times 10^{10}\,\text{L mol}^{-1}\,\text{s}^{-1}] \tag{7}$$

$$O_2^{\bullet -} + NO_2^- + 2H^+ \rightarrow H_2O_2 + {}^{\bullet}NO_2 \quad [k = 5 \times 10^6\,\text{L mol}^{-1}\,\text{s}^{-1}] \tag{8}$$

$$^{\bullet}OH + NO_2^- \rightarrow {}^{\bullet}NO_2 + OH^- \quad [k = 1.0 \times 10^{10}\,\text{L mol}^{-1}\,\text{s}^{-1}] \tag{9}$$

The $^{\bullet}NO_2$ radicals may thus result from various routes (Eqs. (1), (6) and (9)) and at a lesser extent from Eqs. (10) and (11). Their production may be limited by radical duplication (Eqs. (4) and (13)) or inhibited by oxygen (reaction (12) with $O_2^{\bullet -}$ issuing from (7)):

$$2^{\bullet}NO + O_2 \rightarrow 2^{\bullet}NO_2 \quad [2k = 4.2 \times 10^6\,\text{L}^2\,\text{mol}^{-2}\,\text{s}^{-1}] \tag{10}$$

$$NO_3^- + {}^{\bullet}NO \rightarrow {}^{\bullet}NO_2 + NO_2^- \quad [k \leq 4 \times 10^4\,\text{L mol}^{-1}\,\text{s}^{-1}] \tag{11}$$

$$^{\bullet}NO_2 + O_2^{\bullet -} \rightarrow NO_2^- + O_2 \quad [k = 4.5 \times 10^9\,\text{L mol}^{-1}\,\text{s}^{-1}] \tag{12}$$

$$^{\bullet}NO_2 + {}^{\bullet}NO\,(+H_2O) \rightarrow 2NO_2^- + 2H^+ \quad [k = 1.6 \times 10^8\,\text{L mol}^{-1}\,\text{s}^{-1}] \tag{13}$$

Hence, the aim of the present study was to determine the kinetics and pathways of monuron photodegradation induced by nitrate and nitrite ions in water. A special attention was given to the relative reactivity of $^{\bullet}OH$ *versus* $^{\bullet}NO_2$ or $^{\bullet}NO$ through examination of the proportions between their respective products in function of environmental factors.

2. Experimental

2.1. Chemicals

Monuron (3-(4-chlorophenyl)-1-1-dimethylurea, 99.5%) was purchased from Cluzeau-Info-Labo (Ste Foy-la-Grande, France). Sodium nitrate and sodium nitrite (ACS reagent grade) were obtained from Sigma–Aldrich (St Quentin Fallavier, France). HPLC plus grade acetonitrile and RPE methanol were purchased from Carlo Erba (Val-de-Reuil, France). LC-grade water was prepared by purification of reverse osmosis water in an Elgastat UHP system (Elga, High Wycombe, UK). Monuron aqueous solutions were prepared by ultra-sound activated dissolution, followed by filtration through 0.45 μm membrane (Millipore, St Quentin-en-Yvelines, France). When necessary, pH was adjusted by addition of dilute solutions of sulphuric acid or sodium hydroxide (VWR, Fontenay-sous-Bois, France).

2.2. Irradiations

Polychromatic irradiations were performed using a cylindrical device equipped with six lamps (TLD 15 W, Philips) emitting within 300–450 nm with a maximum emission at 365 nm. Light intensity measured by a radiometer (Vilber Lourmat, Marne la Vallée, France) at 312 and 365 nm was 0.18 and 2.4 mW cm^{-2}, respectively. A cooling fan was fitted at the bottom of lamp house to eliminate excess heat. The test solution (300 mL) containing the pesticide and spiked with freshly prepared nitrite/nitrate was placed in a 3 cm i.d. tubular Pyrex reactor at the centre of the lamp housing, with open-top access for sampling. The solution was thoroughly mixed with gas sparging (150 mL min^{-1}). Pure oxygen or nitrogen gas was used as an alternative to air (purging from 20 min before starting irradiation to the end). Samples (1 mL) were taken at selected intervals during the irradiation and analysed by HPLC.

Direct photolysis was performed using 60 mL aqueous solution of the pesticide in a 2 cm i.d. quartz tube, under magnetic stirring and with gas purging as previously. The reactor was positioned parallel to a monochromatic 254 nm low-pressure mercury lamp (germicide TUV 15 W, Philips) with an incident photon flow evaluated as 2.6×10^{15} photons cm^{-2} s^{-1} by ferrioxalate actinometry [20]. Monuron quantum yield and evolution of UV spectrum were determined by irradiation in a 1 cm path length quartz cell with a 6 W low-pressure mercury lamp (Philips) equipped with a metallic cover to allow parallel beam along the 5 cm distance between lamp and cell (incident photon flow 3.7×10^{14} photons cm^{-2} s^{-1}).

2.3. Analytical determinations

Analysis of monuron and its photoproducts was performed by HPLC using a Waters system (600 MS pump equipped with automatic injector 717 and photodiode array UV-detector

991 MS) with a 250 × 4.6 mm i.d. end-capped C_8 Nucleodur, 5 μm particle size, reversed-phase column (Macherey-Nagel, Düren, Germany). The mobile phase was a mixture of water and acetonitrile (75/25 to 50/50 gradient) and the flow rate 1 mL min^{-1}. Absorbance was measured continuously in the range of 200–300 nm and quantifications were carried out at 250 nm with external calibration using monuron as standard (and 1,4-benzoquinone for 254 nm irradiations). The photoproducts were evaluated on the basis of monuron UV-response.

The concentration of nitrite and nitrate ions was determined by HPLC using ion-pairing chromatographic conditions adapted from Ref. [21]. UV spectra were recorded using an Uvikon 933 double beam spectrophotometer (Kontron, Milan, Italy).

For structural determinations, solid phase extraction (SPE) was performed with an Autotrace SPE workstation (Tekmar, Cincinnati, OH, USA) using 120 mg/3 mL Oasis HLB prepacked cartridges (Waters). The SPE supports were preconditioned with 5 mL of methanol and then, 10 mL of water. Typically, 200 mL of photodegraded monuron solution were percolated at 5 mL min^{-1}. After rinsing with 1 mL water, the phase was dried for 15 min under a nitrogen flow and eluted with 2× 2 mL of methanol.

Structural elucidation of SPE concentrated photoproducts was achieved by LC–MS–MS. Samples were injected in a Waters (Alliance 2695) HPLC system coupled to a Quattro LC triple quadrupole mass spectrometer (Micromass, Manchester, UK) with electrospray interface, using positive and/or negative ionization. Data acquisition and processing were performed by MassLynx NT 4.0 system. The electrospray source voltages were: capillary 3.2 kV, extractor 2 V, cone voltage 22 and 17 V, respectively under positive and negative modes. The source block and desolvation gas were heated at 120 °C and 400 °C, respectively. Nitrogen was used as nebulisation and desolvation gas (75 and 450 L h^{-1}, respectively). For MS–MS, collisional induced dissociation (CID) was used with 2.5×10^{-3} mbar argon and 15 eV collision energy.

3. Results and discussions

3.1. Remarks on direct photolysis (254 nm irradiation)

Some experiments were conducted under 254 nm UV irradiation using monuron 50 μM (10 mg/L) pure aqueous solutions. When the reaction was monitored by UV spectroscopy, the initial high absorption at 244 nm was found to decrease and shifting slightly (246.5 nm) whereas a new absorption appeared at 270 nm within a few minutes (Fig. 1). Monuron direct photolysis followed a first order kinetics (k' $4.45 \pm 0.11 \times 10^{-3}$ s^{-1}). Reactivity was even faster (k' $6.33 \pm 0.03 \times 10^{-3}$ s^{-1}, significant difference according to *t*-test with p 0.05) under nitrogen bubbling (absence of oxygen). The quantum yield of disappearance Φ 0.050 ± 0.003 was twice lower than previous values determined using higher monuron concentration and wavelength [22] or methanolic solutions [23]. Three main photoproducts were observed (Fig. 2) in a normally aerated solution. A *N*-substituted iminoquinone **3** appeared rapidly to reach a 32% maximum after 8 min irradiation. This compound then decreased concomitantly

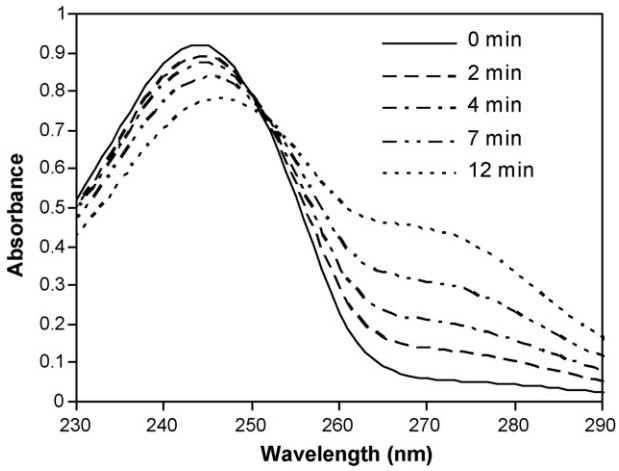

Fig. 1. Evolution of the UV spectrum of a 50 μM solution of monuron irradiated at 254 nm.

with the appearance of 1,4-benzoquinone **3′** yielding an 11.7% maximum at 15 min. A Cl/OH substituted compound **2** was also produced. Its evolution curve appearing with some delay (22.4% max at *ca*. 20 min) indicated a possible filiation from **3** and a higher stability (>15% of **2** remaining after 1 h irradiation). In the absence of oxygen, **3** and **3′** were poorly produced (<3%) whereas **2** becoming the major product gave rise to a plateau corresponding to *ca.* 25–30% of the initial substrate. An

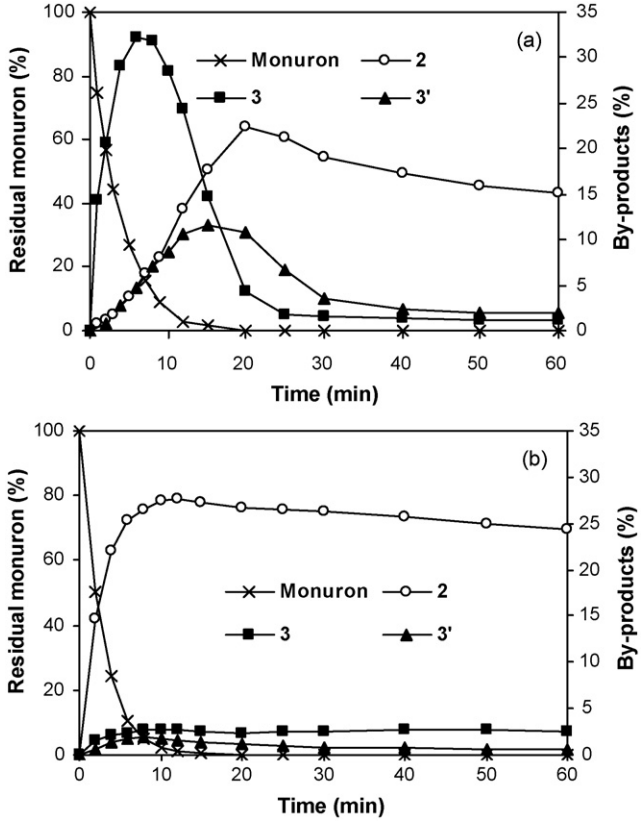

Fig. 2. Evolution curves of monuron (50 μM) and main by-products during direct photolysis at 254 nm: (a) under air and (b) nitrogen purge. By-product numbers according to Scheme 1.

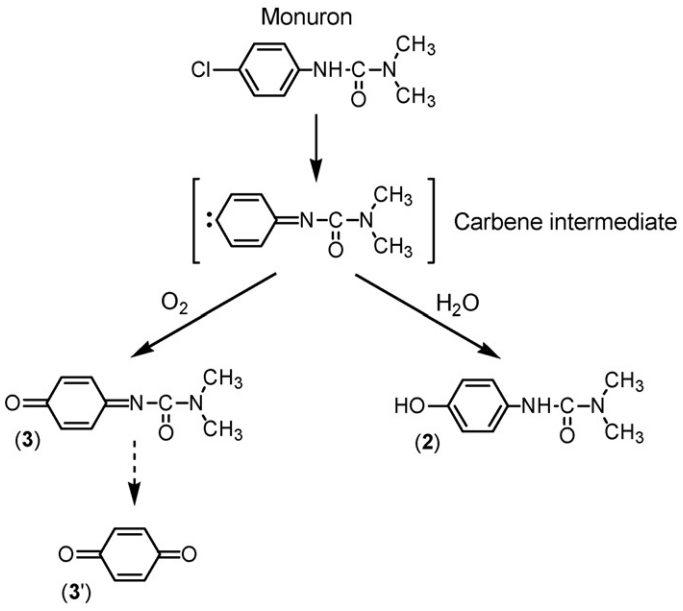

Scheme 1. Pathways of monuron direct photolysis at 254 nm (adapted from [6]).

iminoquinone-like structure was mentioned as unstable intermediate in the photolysis of metobromuron [24]. In the present study, the occurrence of *N*-substituted iminoquinone **3** is clearly established. This compound and subsequent products (particularly through reaction with O_2) should probably originate from a carbene (Scheme 1) as has been suggested in previous studies [6]. The single substituted Cl/OH compound observed in the N_2 conditions would then result from hydrolysis of carbene [6,25]. The acceleration of the degradation of monuron under those conditions further indicates that the photoreaction was partly inhibited by oxygen. A similar effect was observed for monolinuron [14].

3.2. Kinetics of monuron photodegradation induced by nitrates and nitrites

Under 300–450 nm irradiation and without inducer, monuron (MNU) underwent degradation very slowly as expected (<3% in 32 h). However, in the presence of NO_3^- or NO_2^-, induced degradation was found to occur efficiently.

In the case of NO_3^-, the initial disappearance of monuron followed a first-order kinetics (with $R^2 > 0.98$). Kinetics pseudo-constant k' determined for <20% disappearance and degradation rates are listed in Table 1. The k' values were clearly dependent on [NO_3^-], appearing even proportional at $[MNU]_0$ 50 μM (k' 13.0, 5.89 and 1.04×10^{-6} s^{-1} at 10, 5 and 1 mM [NO_3^-], respectively). These results are directly linked to the production rates of the reactive species (*i.e.* mostly •OH). Some proportionality was also observed at $[MNU]_0$ 5 μM except in the 1–5 mM [NO_3^-] interval where the ratio is of a factor 2 only. On the other hand, when considering a constant concentration of the inducer it was noticed that the increase of the substrate concentration from 5 to 50 μM did not give rise to a proportional (but reduced) increase of the degradation rates $k'C_0$. As an example, the ratio was *ca.* 2 at the 1 mM NO_3^- concentration, but *ca.* 4 at 5 mM NO_3^-. This could be explained by a reduced •OH stationary level under high substrate concentrations (the •OH generation rate becoming the limiting factor). The influence of oxygen concentration in water was studied using N_2, air or O_2 as purging gas. The kinetic pseudo-constants were 8.7, 11.4 and 12.8×10^{-6} s^{-1}, respectively, but not significantly different ($n = 3$, *t*-test with p 0.05). Considering the experimental half-lives, the N_2 conditions were found, however, significantly slower as compared to aerated solutions: 19.8 ± 0.8 h *versus* 15.1 and 14.3 ± 2 h for air and O_2, respectively. It means likely that dissolved oxygen is involved in some of the phototransformation processes occurring on the phenylurea. More details will be provided in Section 3.4.

Table 1
Kinetics pseudo-constants k' and initial degradation rates k' $[MNU]_0$ of monuron photodegradation induced by nitrite and nitrate ions under air purge

$[MNU]_0$ (μM)	[Inducer] (mM)	pH	k' ($\times 10^{-6}$ s^{-1})	k' $[MNU]_0$ ($\times 10^{-11}$ mol L^{-1} s^{-1})
Nitrate				
50	10	7	13.0	65.4
50	5	7	5.89	29.8
50	1	7	1.04	5.34
50	0	7	0.04	0.19
5	5	7	13.6	6.96
5	1	7	5.59	2.83
5	0.1	7	0.65	0.33
5	0	7	0.15	0.08
Nitrite				
50	1	7	12.4	60.8
50	1	5	19.9	101
50	1	4.5	38.4	192
50	1	4.3	75.2	383
50	1	3.6	100	500
5	1	7	22.0	11.4
5	0.1	7	20.7	10.7
5	0.01	7	13.4	6.77

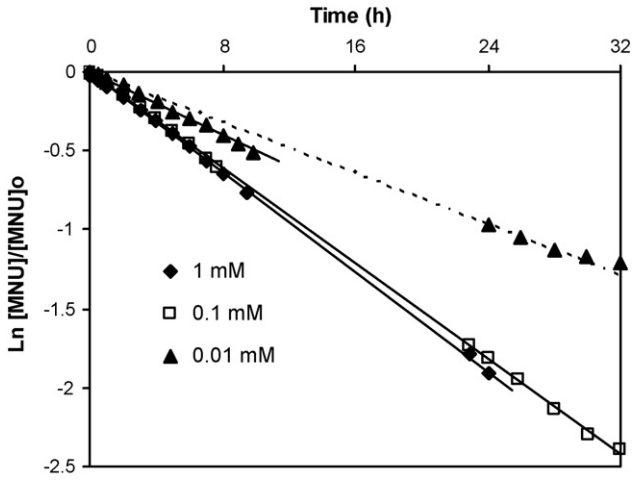

Fig. 3. Kinetics of monuron photo-induced degradation (5 μM) at three NO_2^- concentrations (air sparging, solution pH). Continuous lines represent linear regressions and the dashed line shows absence of linearity.

The effect of nitrite ion concentration on photodegradation kinetics was studied with initial [NO_2^-] ranging from 1 to 0.01 mM for solutions containing 5 μM monuron. The disappearance of monuron followed a first-order kinetics during the whole reaction (not only until 20%). The pseudo-constants k' measured at 1 and 0.1 mM [NO_2^-] were very close (k' 22.0 and 20.7 × 10^{-6} s^{-1}, respectively). This behaviour indicates that with the highest concentration of inducer, the supplement of reagent is used as scavenger towards the produced •OH radicals (Eq. (9)) thus limiting the expected increase of kinetics. On the opposite, k' measured at 0.01 mM [NO_2^-] is much more affected (13.4 × 10^{-6} s^{-1}) as compared to the 0.1 mM concentration. Furthermore, the non-linear evolution of monuron concentration (Fig. 3) observed after 20% degradation should be explained by a higher competition of the photoproducts towards •OH radicals and also by the noticeable decrease of NO_2^- concentration (38% and 85% after 8 h and 32 h, respectively). Dissolved [O_2] level had no significant effect on the kinetics of monuron-induced phototransformation at the highest concentrations of NO_2^- examined (k' *ca.* 20–23 × 10^{-6} s^{-1}). However, as expected, kinetics was highly influenced by the pH. k' values of 12.4, 19.9, 38.4, 75.2 and 100 10^{-6} s^{-1} were observed at pH 7, 5, 4.5, 4.3 and 3.6, respectively. This is due to the NO_2^-/HNO_2 equilibrium (pK_a 3.37) which gives rise to nitrous acid of higher UV absorbance near the lamp maximum emission (365 nm) and superior quantum yield than the NO_2^- species to form •OH radicals [19]. This assumption was confirmed by the absence of reactivity in the dark (<1% degradation in 24 h).

3.3. Identification of the photoproducts

The LC–UV chromatograms obtained in the photo-induced conditions differed significantly whether the reaction was conducted in the presence of NO_3^- or NO_2^- as inducer (Fig. 4). More than 15 photoproducts were identified mostly on the basis of their MS spectra and MS–MS fragmentation pattern in the positive and/or negative mode. A number of them were recog-

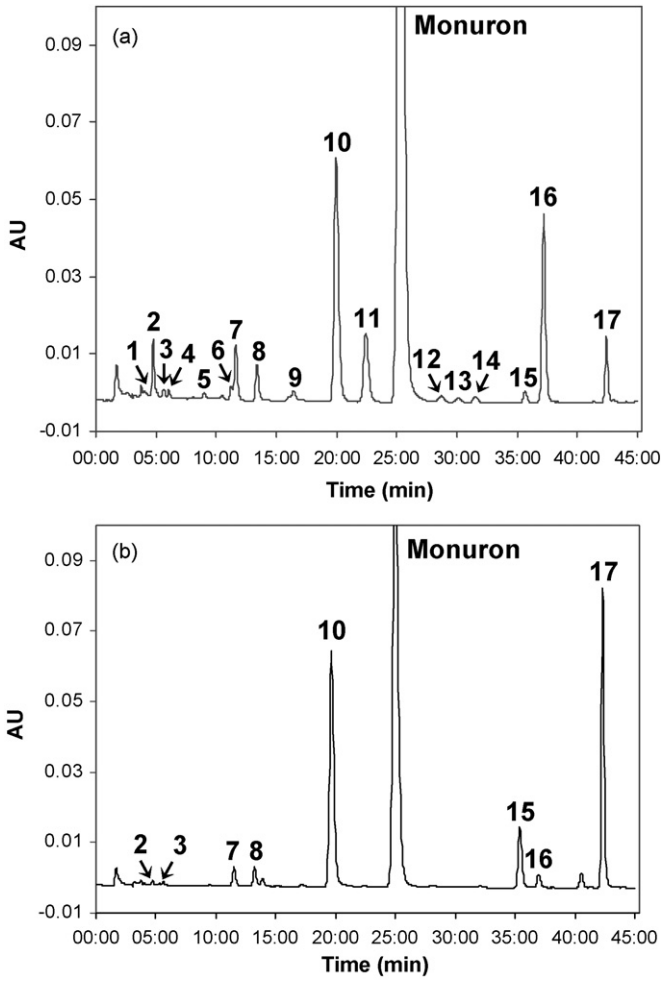

Fig. 4. HPLC–UV chromatogram of the SPE extract of a 32 h-irradiated solution of MNU (50 μM) under air purge in the presence of: (a) 5 mM NO_3^- (65% degradation) and (b) 1 mM NO_2^- (88% degradation). Structures are mentioned in Schemes 1 and 2, except **14** (unknown).

nized after careful comparison with previous studies of our group on phenylurea transformation through advanced oxidation processes (AOPs) which also generate •OH radicals [26] or NO_3^- and NO_2^--induced photodegradation [14,15]. The following data will thus only concern the compounds that are new and/or specific of this work. Thus, the substituted quinone-imine **3** (*cf.* direct photolysis) whose molecular mass 178 was determined by positive MS, was then studied by MS–MS. The CID spectrum of the MH^+ ion *m/z* 179 exhibited ion products at *m/z* 44, 72 and 134 revealing unchanged CO–N(CH_3)$_2$ subunit *versus* monuron and a specific ion at *m/z* 106 [O=C_6H_3=NH]$^+$ resulting from the loss of the formamide OHC–N(CH_3)$_2$. Its UV spectrum showed a high absorption at 269 nm which was that revealed during the UV monitoring of the reaction. Compound **8** was identified, as for other unstable carbinolamines of this type [15 and cited ref.], by its MS spectra yielding either [$MH - H_2O$]$^+$ at *m/z* 197 in the positive mode or [$M - H - CH_2O$]$^-$ at *m/z* 183 in the negative one rather than the corresponding molecular species. The CID spectra of those ions had a behaviour consistent with such structure: loss of •CH_2OH or O=C=NCH_3 leading to ions *m/z* 166 and 140 from [$MH - H_2O$]$^+$ and elim-

ination of O=C=NCH$_3$ from the $[M-H-CH_2O]^-$ anion to yield the anilinure Cl–C$_6$H$_4$–NH$^-$ at *m/z* 126.

Three nitro-derivatives were identified. The first generation product **17** gave simple MS–MS spectra exhibiting a single product ion at *m/z* 72 $[O=C=N(CH_3)_2]^+$ when starting from the MH$^+$ ion at *m/z* 244 and a prominent anion at *m/z* 46 corresponding to NO_2^- for the $[M-H]^-$ parent ion *m/z* 242. Compounds **15** and **7** yielded more complex CID spectra for their $[M-H]^-$ ion. Ion *m/z* 228 (from **15**) produced a fragment at *m/z* 171 by loss of O=C=NCH$_3$ (57 u) itself dissociable into ions *m/z* 46 $[NO_2]^-$ and 141 $[171-NO^\bullet]^{-\bullet}$ among others when carrying out a *pseudo*-MS^3 experiment. The deprotonated molecule *m/z* 224 obtained from **7** gave directly an ion at *m/z* 194 by loss of NO$^\bullet$ together with product ions at *m/z* 179, 150 and 136 indicating the conservation of the urea function. The hydroxylated compounds **11** and **6** gave similar MS–MS spectra. **6** had the same retention time as one of the Cl/OH substituted derivatives issuing from diuron [15] and was thus assumed to be the *meta* isomer with respect to the urea.

3.4. Evolution of the photoproducts as a function of the environmental parameters

The production of the photoproducts was clearly influenced by some of the environmental factors.

3.4.1. Oxygen concentration

Under 5 mM NO_3^- photo-induced degradation, the main effect of reducing dissolved oxygen using nitrogen purge was that nitration almost did not occur. The highest yield of nitro-derivative of MNU **17** was thus obtained under aerated conditions (Fig. 5c). Furthermore, this compound was relatively stable since only poorly transformed into second-generation products (*cf.* **7** and **15**). The necessary involvement of O_2 to produce nitration seems in favour of a two-step pathway such as that suggested in some conditions of photonitration of phenol, *i.e.* through $^\bullet NO_2$ addition and H$^\bullet$ abstraction by O_2 [27]. The formation of products resulting from the oxidation of the N-terminus group differed mainly (Fig. 5a) by a much lower yield of the N–CH$_3$CHO derivative **16** in the absence of O_2. This effect was partly counterbalanced by a significantly higher production of *N*-demethylated (NHCH$_3$) MNU (**10**). The necessary role of oxygen in the formation of *N*-formyl derivatives from such phenylureas has already been emphasized [15]. In contrast, the route that produces successively the carbinolamine **8** and compound **10** depends only upon reactions with $^\bullet$OH radicals. Comparison of the profiles obtained for the Cl/OH substituted derivative **2** (Fig. 5b) indicated a progressive increasing level from the oxygen to the nitrogen (*via* air) conditions, reminding the direct photolytic behaviour (*cf.* 3.1.) and thus suggesting a contribution of this process. However, the parallel evolution of the substituted imino-quinone **3** which also occurred in the NO_3^--induced photodegradation conditions was not clearly explained. Under the NO_2^- conditions, the yields of the N-terminus group oxidation products **8** and **10** were found to increase when increasing the oxygen content (Fig. 6). This

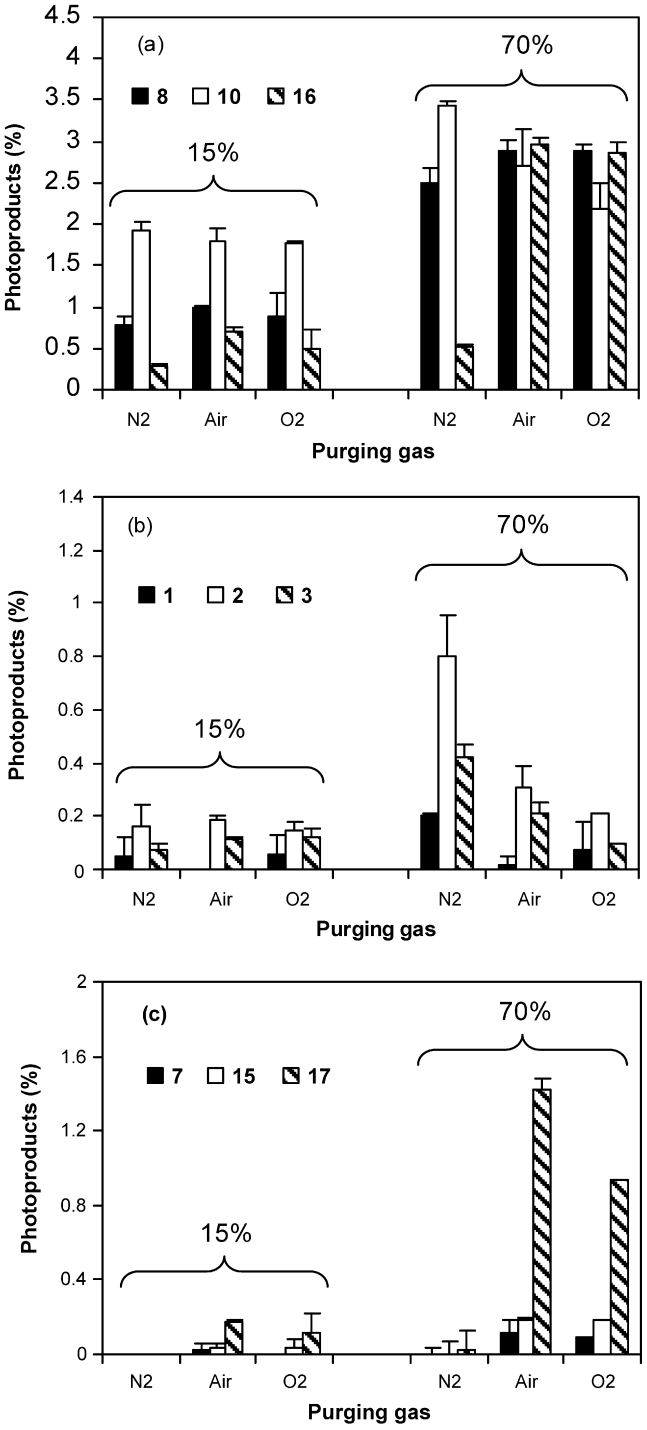

Fig. 5. Effect of oxygen concentration on the accumulated photoproducts of monuron NO_3^--induced photodegradation at 15% and 70% degradation ($[MNU]_0$ 50 μM, NO_3^- 5 mM, neutral pH): (a) N-terminal degradation, (b) Cl/OH substitution and (c) phenyl nitration (numbers in legends refer to the photoproducts according to Fig. 4 and Scheme 2).

effect was particularly visible at 70% degradation. An inverse tendency was observed as for nitrated-MNU **17**.

3.4.2. Inducer concentration

An effect of NO_3^- concentration on the evolution curves (not shown) of the photoproducts was clearly evidenced in the

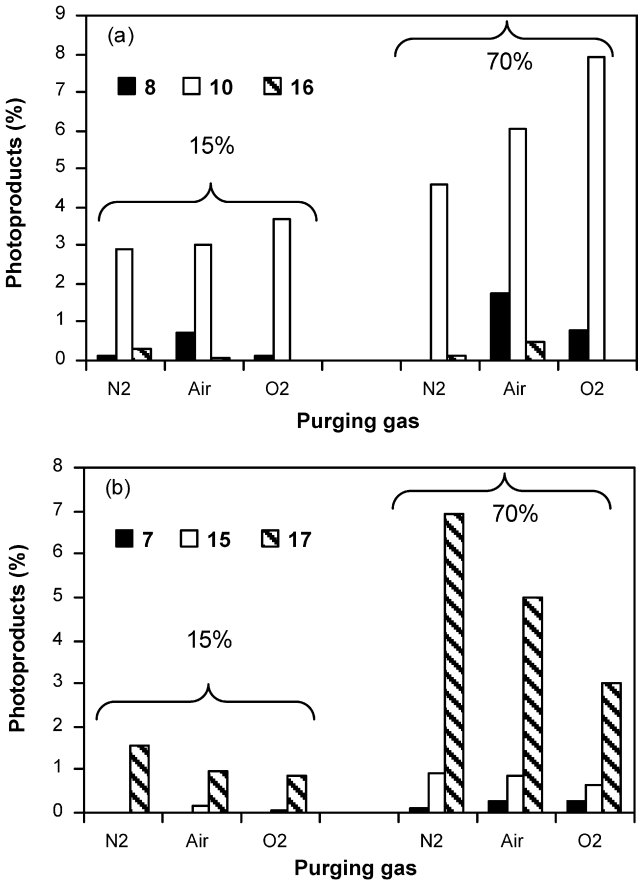

Fig. 6. Effect of oxygen concentration on the accumulated photoproducts of monuron NO_2^--induced photodegradation at 15% and 70% degradation ([MNU]$_0$ 50 μM, NO_2^- 1 mM, neutral pH): (a) N-terminal degradation and (b) phenyl nitration (numbers in legends refer to the photoproducts according to Fig. 4 and Scheme 2).

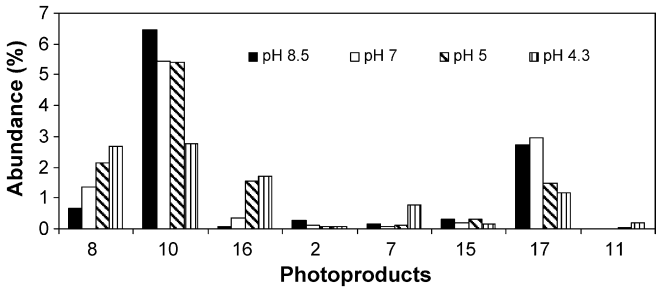

Fig. 7. Effect of pH on the accumulated photoproducts (numbered according to Fig. 4 and Scheme 2) of monuron NO_2^--induced photodegradation at 40% degradation ([MNU]$_0$ 50 μM, NO_2^- 1 mM, air).

1–10 mM range. This was mostly due to the different advancement rates of the degradation (14%, 65% and 88% after 32 h for 1 mM, 5 mM and 10 mM NO_3^-, respectively). However, a subsequent degradation of some of the photoproducts (**8**, **10** and **11**) could be noticed when using the highest concentration, whereas all of them were continuously accumulating in the low concentration conditions. The same kind of behaviour was observed with NO_2^- in the 0.01–1 mM interval of concentration (compounds **2** and **10** being further degraded in the two latter concentrations). The nitro-derivative **17** was produced at a significantly higher level at 0.1 mM NO_2^- (*ca*. 2.2% *versus* 1.5% after 24 h).

3.4.3. *Effect of pH*

The pH greatly influenced the kinetics of degradation of MNU under the NO_2^-conditions especially when approaching its pK_a value. Concomitantly, it was observed that the carbinolamine **8** and the *N*-formyl urea **16** were obtained in higher yields at pH 4–5 whereas the *N*-demethylated MNU **10** level was significantly reduced (Fig. 7). Inversely, nitration (*cf*. **17**) was found less favoured at low pH values. When considering combined effects, it was noticed that at such pHs the formation of the

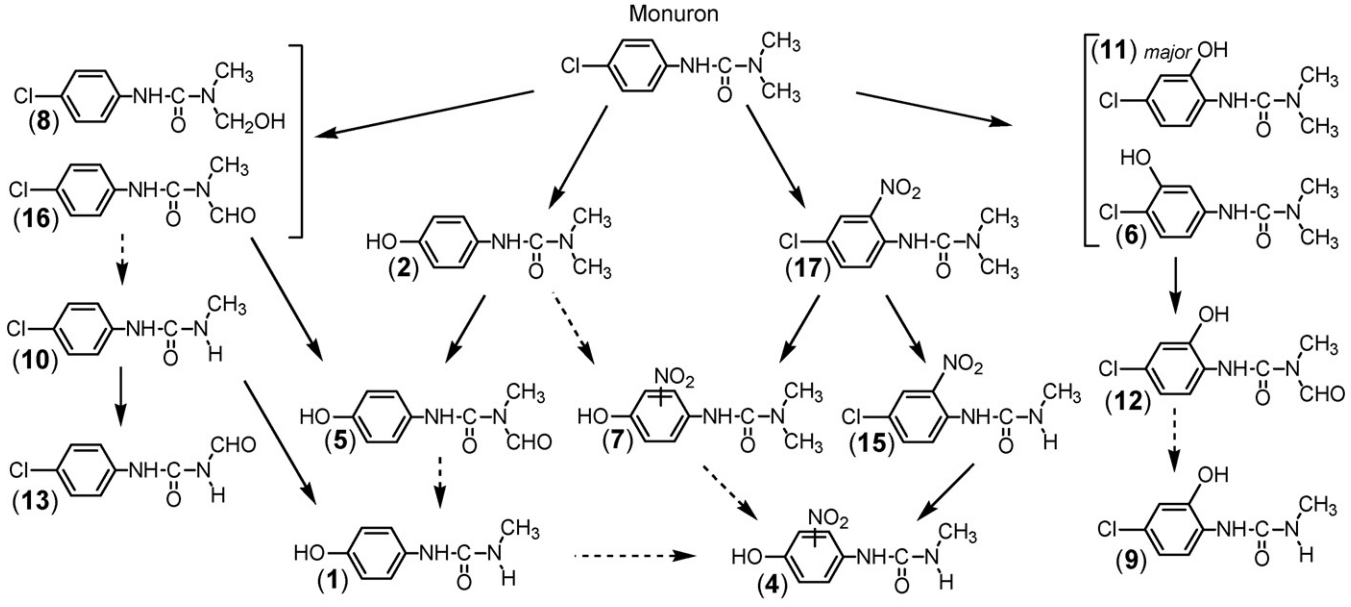

Scheme 2. Pathways of monuron photo-induced degradation by NO_3^- and NO_2^- (iminoquinone **3**, also formed in this context, is not presented).

N-terminus oxidation products **10** and **16** was favoured by the presence of oxygen (data not shown). The nitro-compounds **17**, **15** and **7** were also more produced in such conditions.

3.5. Degradation pathways: contribution of photonitration

Both inducers led to close results in terms of photoproducts, but not in proportions. Furthermore, the latter were influenced differently by the environmental parameters. Four main pathways could be considered: (i) reaction of $^{\bullet}$OH on the methyl groups of the urea function or (ii) on the aromatic ring, (iii) Cl/OH substitution and (iv) the reaction of a nitrogen species on the phenyl ring to produce nitration (Scheme 2).

The N-terminus group oxidation pathway (*cf.* compounds **8**, **10** and **16**) was the major one in abundance under the NO_3^--induced conditions. The three other pathways were also present. The Cl/OH substitution (yielding **2** and subsequent products) might occur either by $^{\bullet}$OH-mediated reaction or by direct photolysis as demonstrated by the simultaneous formation of the imino-quinone product **3**. This compound was, however, produced at trace level, which was in agreement with the very low UV absorption of MNU in the 300–450 nm region. Ring hydroxylation was also observed leading predominantly to the *ortho* isomer with respect to the urea (**11** and its derivatives **9** and **12**) *versus* the *meta* one (**6**). Such orientation of the $^{\bullet}$OH electrophilic attack onto the phenyl ring is in agreement with the global electron-donating effect of the urea and the minor opposite effect of the chlorine. Photonitration was produced competitively and regiospecifically (*ortho* isomer only) under aerated conditions. The nitro-phenylurea **17** represented approximately half the yield of each N–$(CH_3)_2$ oxidation product (Fig. 5). Under NO_2^- conditions, the induced photodegradation of MNU was less diverse producing mostly *N*-monodemethylated MNU **10** (first pathway) and nitration products (**17** major, and second-generation products **15** and **7** issuing from the former by demethylation and Cl/OH substitution, respectively). These more drastic conditions as compared to NO_3^- (at a five-fold higher concentration) may explain the less detected hydroxylated molecules (carbinolamine **8** and ring OH-substituted derivatives) likely degraded rapidly whenever formed. The higher yield of nitration (ca. three-fold, Fig. 8) in the presence of irradiated NO_2^- is not surprising. It was clear also that this reaction occurred under a different mechanism than with NO_3^- as inducer according to the observed oxygen effect. Nitration of the phenyl ring was thus likely due to an electrophilic attack of N_2O_4 [28], oxygen when present playing a limited inhibiting role (Eqs. (12) and (4)). Further, a contribution of a $^{\bullet}$NO (or N_2O_3)-mediated reaction in the aerated conditions [28,29] could be considered as negligible since none nitroso-derivative was detected as intermediate. Under NO_3^- irradiated conditions, a pathway involving an initial attack by the $^{\bullet}NO_2$ radical followed by a reaction with O_2 should be dominating, since no nitration occurred in the absence of oxygen (Scheme 3). Such reactivity strongly differs from that of phenol in similar NO_3^- or NO_2^- environment [27–29].

As shown in Fig. 8, the proportions of the different pathways are also highly dependent on the phenylurea structure. Changing the N-terminus group into $N(CH_3)OCH_3$ (*cf.* monolinuron [14]) will have some incidence on the kinetics of degradation and the proportions of the photoproducts. The introduction of a second chlorine atom as ring substituent (*cf.* diuron [15]) will strongly reduce the nitration content in both NO_2^- and NO_3^- conditions due to an increase of the electron-withdrawing effect on the phenyl ring. Instead, the introduction of a methyl group (electron-donating) like for chlortoluron will give an opposite effect [unpublished]. Fe(III)-induced photodegradation of monuron was also characterized [12] by the production of N-terminus oxidation and ring-hydroxy products. Mineralization was observed too that might also occur in our case according to the low mass balances obtained.

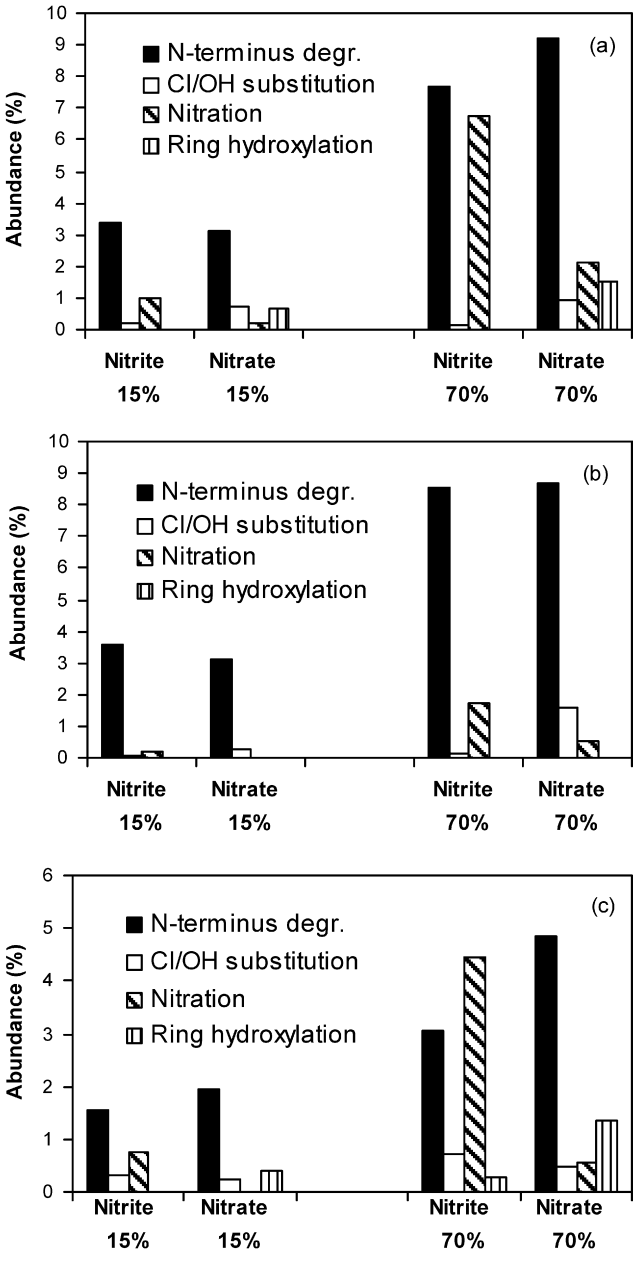

Fig. 8. Distribution of the four main pathways at 15% and 70% degradation in the presence of 1 mM NO_2^- or 5 mM NO_3^- (50 μM, neutral pH, air): (a) monuron, (b) diuron and (c) monolinuron.

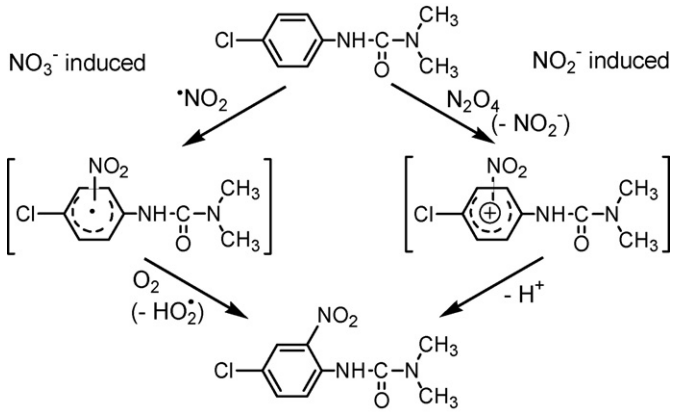

Scheme 3. Proposed mechanisms for monuron photonitration induced by NO_3^- and NO_2^-.

4. Conclusions

Monuron was found to be efficiently photodegraded in the presence of NO_3^- and NO_2^-. The importance of this degradation was shown to vary according to experimental parameters (dissolved oxygen, pH, monuron and inducer concentration). In the environment, these parameters may play an important role, but some other constituents present in natural waters such as bicarbonate ions, organic matter or iron content may also contribute to the phototransformation process [30,31]. Numerous photoproducts have been characterized using LC–MS–MS, revealing four major pathways involved together with a minor contribution of direct photolysis. Reactive species are produced in both NO_3^- and NO_2^- conditions generating oxidative degradation of the N-terminus group, but also competitive hydroxylation and nitration of the phenyl ring. Such competition is particularly visible in the presence of the nitrate ion even at low "environmental" concentrations. The toxicity of nitroderivatives of MNU (and analogues) as potent contaminants should be investigated on aquatic organisms and evaluated for risk assessment.

Acknowledgements

INRA is acknowledged for a postdoc fellowship to one of us (MVS). X. Li is thanked for his contribution at the beginning of the study.

References

[1] J.W. Eichelberger, J.J. Lichtenberg, Environ. Sci. Technol. 5 (1971) 541–544.
[2] P.W.M. Augustijn-Beckers, A.G. Hornsby, R.D. Wauchope, Rev. Environ. Contam. Toxicol. 137 (1994) 1–82.
[3] S.R. Sørensen, G.D. Bending, C.S. Jacobsen, A. Walker, J. Aamand, FEMS Microbiol. Ecol. 45 (2003) 1–11.
[4] D. Sabaliūnas, J. Ellington, R. Lekevičius, Int. J. Environ. Anal. Chem. 64 (1996) 123–134.
[5] D.G. Crosby, C.S. Tang, J. Agric. Food Chem. 17 (1969) 1041–1044.
[6] A. Boulkamh, C. Richard, New J. Chem. 24 (2000) 849–851.
[7] F.S. Tanaka, R.G. Wien, B.L. Hoffer, J. Agric. Food Chem. 30 (1982) 957–963.
[8] F.S. Tanaka, R.G. Wien, E.R. Mansager, J. Agric. Food Chem. 27 (1979) 774–779.
[9] P.H. Mazzocchi, M.P. Rao, J. Agric. Food Chem. 20 (1972) 957–959.
[10] E. Pramauro, M. Vincenti, V. Augugliaro, L. Palmisano, Environ. Sci. Technol. 27 (1993) 1790–1795.
[11] M. Bobu, S. Wilson, T. Greibrokk, E. Lundanes, I. Siminiceanu, Chemosphere 63 (2006) 1718–1727.
[12] H. Měšťánková, G. Mailhot, J.F. Pilichowski, J. Krýsa, J. Jirkovský, M. Bolte, Chemosphere 57 (2004) 1307–1315.
[13] C. Richard, D. Vialaton, J.P. Aguer, F. Andreux, J. Photochem. Photobiol. A: Chem. 111 (1997) 265–271.
[14] S. Nélieu, L. Kerhoas, M. Sarakha, J. Einhorn, Environ. Chem. Lett. 2 (2004) 83–87.
[15] M.V. Shankar, S. Nélieu, L. Kerhoas, J. Einhorn, Chemosphere 66 (2007) 767–774.
[16] P. Warneck, C. Wurzinger, J. Phys. Chem. 92 (1988) 6278–6283.
[17] D. Vione, V. Maurino, C. Minero, E. Pelizzetti, in: P. Boule, D.W. Bahnemann, P.K.J. Robertson (Eds.), The Handbook of Environmental Chemistry—Environmental Photochemistry Part II, Springer, Berlin, 2005, pp. 221–253 (and references therein).
[18] R.J. Kieber, A. Li, P.J. Seaton, Environ. Sci. Technol. 33 (1999) 993–998.
[19] M. Fischer, P. Warneck, J. Phys. Chem. 100 (1996) 18749–18756.
[20] J.G. Calvert, J.M. Pitts, Photochemistry, Wiley, New York, 1996, pp. 783–786.
[21] J. Threeprom, S. Watanesk, R. Watanesk, P. Kijjanapanich, P. Wiriyacharee, R.L. Deming, Anal. Sci. 18 (2002) 947–950.
[22] F.S. Tanaka, R.G. Wien, R.G. Zaylskie, J. Agric. Food Chem. 25 (1977) 1068–1072.
[23] K. Nick, H.F. Schöler, Vom Wasser 86 (1996) 57–72.
[24] A. Boulkamh, T. Sehili, P. Boule, J. Photochem. Photobiol. A: Chem. 143 (2001) 191–199.
[25] P. Boule, L. Meunier, F. Bonnemoy, A. Boulkamh, A. Zertal, B. Lavedrine, Int. J. Photoenergy 4 (2002) 69–78.
[26] L. Amir Tahmasseb, S. Nélieu, L. Kerhoas, J. Einhorn, Sci. Tot. Environ. 291 (2002) 33–44.
[27] D. Vione, V. Maurino, C. Minero, M. Vincenti, E. Pelizzetti, Chemosphere 44 (2001) 237–248.
[28] D. Vione, V. Maurino, C. Minero, E. Pelizzetti, Chemosphere 45 (2001) 893–902.
[29] F. Machado, P. Boule, J. Photochem. Photobiol. A: Chem. 86 (1995) 73–80.
[30] M.W. Lam, K. Tantuco, S.A. Mabury, Environ. Sci. Technol. 37 (2003) 899–907.
[31] A.C. Gerecke, S. Canonica, S.R. Muller, M. Scharer, R.P. Schwarzenbach, Environ. Sci. Technol. 35 (2001) 3915–3923.